Optimization of Biodiesel Production from Jatropha curcas Oil: Effects of Transesterification Parameters and Gamma Irradiation on Fuel Properties

Mohamed Osman

osman@ioc.ac.ru

ZIOC: FGBUN Institut organiceskoj himii imeni N D Zelinskogo Rossijskoj akademii nauk https://orcid.org/0000-0003-4662-062X

Suleiman A. G. Naser

Omdurman Islamic University

Research Article

Keywords: Biodiesel, Jatropha curcas, Gamma irradiation, Fuel optimization

Posted Date: October 25th, 2025

DOI: https://doi.org/10.21203/rs.3.rs-7590978/v1

Version of Record: A version of this preprint was published at Waste and Biomass Valorization on February 23rd, 2026. See the published version at https://doi.org/10.1007/s12649-026-03539-6.

Abstract

This study investigates the production and enhancement of biodiesel from *Jatropha curcas* oil through transesterification and gamma irradiation. Mature seeds were collected from Sudan, and oil was extracted and characterized for physicochemical properties. Transesterification was optimized by varying methanol-to-oil ratios, catalyst concentrations, reaction time, and temperature, achieving a maximum biodiesel yield of 97% under optimal conditions (30g methanol, 0.5g NaOH, 70°C, 60 min). The biodiesel was further treated with gamma irradiation (3–20 kGy) to assess its impact on fuel properties. Results showed that moderate irradiation (6–10 kGy) improved viscosity, cetane number (peaking at 57), and oxidative stability, while higher doses led to degradation. Key fuel properties, including density, flash point, and ash content, complied with ASTM standards. The study demonstrates that optimized transesterification combined with controlled gamma irradiation enhances biodiesel quality, making *Jatropha curcas* a viable non-edible feedstock for sustainable biofuel production.

Introduction

In recent years, the global population has grown exponentially, leading to a sharp rise in fossil fuel consumption. This escalating demand underscores the urgent need for sustainable and economically viable renewable energy sources [1]. Biodiesel offers several advantages compared to conventional diesel fuel. As a renewable energy source, it generates fewer harmful emissions, exhibits low toxicity due to its biodegradability, and can be produced locally making it particularly beneficial for rural economic development [2–4]. Despite these benefits, biodiesel production faces significant challenges, including high feedstock costs and the need for adaptable processing technologies to efficiently convert various raw materials into fuel [5].

Vegetable oils and animal fats can be transformed into diesel compatible fuels through four primary methods: direct blending, micro-emulsification, pyrolysis, and transesterification [6]. Among these, transesterification is the most widely adopted due to its ability to produce high-quality biodiesel. This process converts triglycerides into alkyl esters, significantly reducing viscosity to match conventional diesel standards. Transesterification can be performed using different techniques, each with distinct advantages, limitations, and ideal feedstock requirements [7]. Critical reaction parameters must be carefully optimized for efficient biodiesel synthesis, including [8–9]: (i) Alcohol-to-oil molar ratio; (ii) Catalyst type and concentration; (iii) Reaction temperature and duration; (iv) Solvent selection and quantity; (v) Reaction medium conditions. By controlling these variables, the process can be tailored to maximize yield and fuel quality across diverse feedstocks.

Biodiesel demonstrates superior environmental performance relative to conventional diesel, characterized by zero sulfur emissions, reduced carbon monoxide output, lower particulate matter, decreased smoke formation, and diminished hydrocarbon emissions. Its higher oxygen content promotes more complete combustion, resulting in overall cleaner exhaust emissions [10–11]. The transesterification process for biodiesel production can occur through both catalyzed and non-catalyzed pathways. Conventional catalytic methods include: *(i)* Chemical catalysis (acid or base-catalyzed reactions); *(ii)* Biochemical catalysis (using lipase enzymes); (iii) Emerging catalytic approaches showing promising results involve nano-catalysts and ionic liquid catalysts. Moreover, Non-catalyzed transesterification employs supercritical alcohol conditions, typically using methanol at temperatures and pressures exceeding its critical point [12–14]. Under these supercritical conditions, the alcohol's dielectric constant decreases significantly, creating a single-phase reaction system that eliminates the typical oil-alcohol immiscibility problem and enhances reaction efficiency [15].

Bhansali and Bhagat [16] conducted a significant investigation into Furfural-Diethyl-Acetal (FDA) as a biofuel additive for gasoline, utilizing metal-free porphyrin photocatalysis under visible light conditions. Their research demonstrated FDA's exceptional performance as a fuel additive, with both 15% and 20% (v/v) gasoline blends maintaining comparable physicochemical properties to pure gasoline, including octane rating and calorific value. Moreover, in our previous research [17], we focused on optimizing the transesterification process for *Jatropha curcas L.* biodiesel production using natural zeolite catalysts. The study further explored enhancing biodiesel quality through furfural-based additives as a sustainable alternative to conventional improvers like thermally unstable 2-ethylhexyl nitrate and other potentially toxic compounds [17]. In addition, in our previous investigation into gamma irradiation's effects on petro-diesel, we identified 15 kGy as the optimal dose for improving physicochemical properties while maintaining ASTM compliance. The study revealed a dose-dependent response in cetane number (CN) enhancement: irradiation at 3 kGy increased CN from 51.4 to 52.7, with further improvements to 53.7 at 6 kGy and 54.2 at 15 kGy. Notably, we observed a non-monotonic relationship, as CN decreased at the intermediate 10 kGy dose, suggesting a complex radiation interaction mechanism. These findings demonstrate gamma irradiation's potential for diesel fuel modification, with 15 kGy emerging as the most effective treatment parameter.

This study systematically optimized transesterification parameters for *Jatropha curcas L.* (non-edible) oil using homogeneous catalytic system. Furthermore, we developed an innovative dual-approach enhancement strategy of gamma irradiation as a post-production modification technique. These eco-conscious methodologies collectively address both production efficiency and fuel quality improvement while adhering to green chemistry principles.

Materials and Methods

Sample Collection

Mature seeds of *Jatropha curcas L*. were collected from wild-growing plants in the Ad-Damazin region of Blue Nile State, Sudan. The plant material underwent formal taxonomic authentication at the Medicinal and Aromatic Plants Research Institute (MAPRI) of Sudan's National Center for Research (NCR), where voucher specimens were deposited for reference.

Physicochemical Properties of Jatropha Oil

The physicochemical properties of *Jatropha curcas* oil were analyzed following standardized methods established by the American Oil Chemists' Society (AOCS) for edible oils. Key parameters assessed included refractive index, moisture content, ash content, kinematic viscosity, density, saponification value, iodine value, peroxide value, acid value, and free fatty acid (FFA) composition [17].

Transesterification Reaction

A 250 mL Erlenmeyer flask was charged with 10 g of jatropha oil, followed by the addition of a methanolic potassium hydroxide solution prepared by dissolving 0.5 g of KOH in 30 mL of methanol. The resulting mixture was stirred at 30°C for 3 hours. After completion of the reaction, the contents were transferred to a separatory funnel, and excess methanol was introduced. To eliminate water-soluble byproducts from the biodiesel layer, it was washed three times with 10 mL portions of a saturated sodium chloride solution (5 M). The pH of the aqueous phase was monitored after each wash, and washing continued until the aqueous layer reached neutrality [18]. A final rinse with 10 mL of distilled water was performed and discarded. To remove residual moisture, the biodiesel was treated with 4 g of magnesium sulfate for 20 minutes and then filtered. It should be noted that all reagents were thoroughly dried prior to the transesterification reaction to prevent saponification.

To optimize the transesterification procedure, we experimented with various methanol-to-oil ratios and catalyst loadings. Furthermore, we examined how reaction time and temperature influenced the biodiesel yield: (i) Time optimization was performed at a constant temperature of 70°C using varying reaction times. (ii) Temperature optimization was assessed across a range of 30–140°C, with each reaction lasting 60 minutes to evaluate thermal effects on the output. The outcomes of these parametric studies are presented in Table 1, offering insights into the optimal conditions for maximizing biodiesel production efficiency.

Gas chromatography-mass spectrometry (GC-MS) provides a robust analytical technique for quantifying fatty acid methyl esters (FAMEs) and detecting residual impurities such as methanol, glycerol, and unreacted triglycerides.

Qualitative analysis of the biodiesel samples was conducted on a Shimadzu GCMS-QP 2010 Ultra Plus system equipped with an AOC-20i/s autosampler and a Thermo Scientific™ TRACE™ TR-WaxMS capillary column. Data acquisition and processing were managed using GCMS Solutions software (Version 4.11 SU2) with support from commercial mass spectral libraries. Samples were introduced via a 0.2 µL injection in split mode (1:10 ratio) with the injector maintained at 250°C. The GC oven temperature program was set as follows: initial temperature 150°C, increased to 250°C at 25°C/min, then raised to 253°C at 1°C/min, followed by a ramp to 275°C at 25°C/min, and finally held at 275°C for 2 minutes. High-purity helium was used as the carrier gas at a constant flow rate of 13 mL/min and an inlet pressure of 99.5 kPa. Biodiesel yield was determined using the equation:

$$Yield\,(\%) = \left(\frac{Total\,FAME\,quantified\,(g)}{Theoretical\,maximum\,FAMEs(g)}\right) \times 100 \quad \text{Eq. 1}$$

where the theoretical FAME content was calculated based on the initial oil weight, triglyceride content, and molecular weights of the reactants. Selectivity toward specific FAMEs was assessed as:

$$Selectivity\,(\%) = \left(\frac{Yield\,of\,target\,FAME}{Yield\,of\,biodiesel}\right) \times 100 \quad \text{Eq. 2}$$

Physicochemical Characterization of Biodiesel

The synthesized biodiesel was analyzed using standardized ASTM methods. Density (D4052) was determined via an oscillating U-tube densitometer, correlating frequency shifts with sample mass. Kinematic viscosity (D7042) was measured by timing gravity-driven flow through a calibrated capillary viscometer. For flash point (D93), a brass cup filled with biodiesel was heated while periodically applying an ignition source until detectable flash occurred. Cloud point (D5773) employed Peltier cooling to identify wax crystallization onset, recorded to 0.1°C precision. Color (D1500) assessment compared samples against standardized glass disks under controlled lighting. Ash content (D482) involved ignition at 775°C to isolate incombustible residues, while water content (D95) used azeotropic distillation with a solvent trap. Carbon residue (D4530) quantified coke formation after pyrolysis under nitrogen at 500°C. Sulfur content (D5453) utilized UV fluorescence of combusted SO_2. Copper strip corrosion (D130) evaluated reactivity by immersing polished copper in heated biodiesel for 2 hours. Cetane number (D6131) derived from ignition delay comparisons against reference fuels in a compression ignition engine.

Elemental Analysis of Jatropha Oil and Biodiesel by ICP

The elemental composition of Jatropha oil and biodiesel was analyzed using ICP under optimized conditions: RF power (750–1500 W), plasma gas flow (12–16 L/min Ar), auxiliary gas (0.3–1.2 L/min Ar), and nebulizer flow (0.3–2.5 L/min Ar). Samples were microwave-digested in HNO_3, and calibration was performed using NIST-traceable standards. Key elements (Na, K, Ca, Mg, P, Fe, Cu, Ni, Zn) were quantified with internal standardization (Y/Sc) and triplicate measurements (RSD < 5%). Critical parameters included exhaust pressure (101.225 kPa), sampler cone pressure (1.32×10^{-3} atm), and ambient temperature (297 K), ensuring precise detection of metal impurities affecting fuel quality (ASTM D7111) [19].

Exposing Biodiesel Sample to Gamma Irradiation

The biodiesel samples underwent gamma irradiation treatment using a Cobalt-60 gamma cell (Model B(U)) in batch processing mode. Irradiation was conducted at ambient temperature (25 ± 2°C) with six progressively increasing absorbed dose levels: 3, 6, 10, 15, 18, and 20 kGy. The corresponding dose rates for these treatments were 2.27, 4.5, 7.4, 11.15, 14.1, and 16.8 kGy/h respectively. For consistent irradiation exposure, prepared samples were placed in 500 mL glass vials filled to capacity to minimize headspace effects. The gamma cell's Cobalt-60 source (1.25 MeV gamma photons) provided uniform dose distribution throughout the sample volume. This batch irradiation methodology ensured reproducible treatment conditions across all test specimens while maintaining controlled environmental parameters.

Results and Discussion

The oil yield from Jatropha seeds was determined to be 28.9% by weight. A comprehensive analysis of the oil's physicochemical characteristics, including moisture content (X%), ash content (X%), density (X g/cm³), refractive index (X at 40°C), peroxide value (X meq/kg), kinematic viscosity (X mm²/s), saponification value (X mg KOH/g), iodine value (X g I_2/100g), and acid value (X mg KOH/g), has been detailed in our previous publication [17]. These analytical findings demonstrate that Jatropha oil possesses suitable properties for biodiesel production, particularly as its characteristics fall outside the edible oil standards established by the WHO [17]. This non-food status addresses concerns about potential competition between biodiesel feedstocks and food supplies. The oil's specific properties, notably its viscosity or acid value, make it particularly favorable for conversion to biodiesel while avoiding conflicts with food security priorities.

Table 1. Effect of Methanol-to-Oil Ratio and Catalyst Loading on Biodiesel Yield at 70°C for 60 minutes					
Reaction Code	Weight of Oil, g	Weight of MeOH, g	Weight of Catalyst, g	Wt. Ratio Oil: MeOH: NaOH	Biodiesel Yield (%)
B1	10	5	0.1	1:0.5:0.01	72
B2	10	10	0.1	1:1:0.01	75
B3	10	15	0.1	1:1.5:0.01	80
B4	10	20	0.1	1:2: 0.01	82
B5	10	25	0.1	1:2.5:0.01	82
B6	10	30	0.1	1:3:0.01	90
B7	10	30	0.5	1:3:0.05	97
B8	10	30	0.75	1:3:0.08	96
B9	10	30	1.25	1:3:0.13	96
B10	10	30	1.5	1:3:0.15	95
B11	10	30	2	1:3:0.2	95
B12	10	30	5	1:3:0.5	95
B13	10	30	7	1:3:0.7	95
B14	10	30	9	1:3:0.9	94
B15	10	30	10	1:3:1	94

Table 1 presents the results of the transesterification reaction optimization. Initial reactions (B1–B6) examined the impact of the MeOH content while keeping the catalyst's weight constant. The detected increase in biodiesel % from 72-90% with increasing methanol from 5-30g can be explicated by the the principles of chemical equilibrium. Rendering to Le Chatelier's principle, adding more MeOH to the biodiesel production reaction should lead to more FAMEs formation. In the same way, the experiment showed that after 30g of MeOH, adding more didn't increase the yield. This suggests the reaction hits a limit where extra methanol doesn't help. This could be because it's harder for the reactants to mix properly due to the mass transfer limitations or because glycerol, a byproduct, dissolves more in the methanol, hindering the reaction.

In the second set of experiments (B6-B15), the we focused on finding the best amount of catalyst, using the ideal methanol amount we found earlier. A big jump in yield (from 90% to 97%) has been observed when we increased the catalyst from 0.1g to 0.5g, suggesting the initial amount wasn't enough for the reaction to fully complete. However, after 0.5g, adding more catalyst didn't make much of a difference. This could be because of the too much base catalyst might cause unwanted saponification reactions [22]. Moreover, the best conditions we found (30g of methanol and 0.5g of catalyst) strike a good balance. In the meanwhile, we avoid using too much MeOH or catalyst, which would cost more money and be worse for the environment. Therefore, it's a good balance of efficient reaction and practical attentions.

The yields' stability at larger catalyst loadings (94–97% for B7–B15, respectively) indicates that additional factors such as the triglyceride molecules' inherent reactivity or the reaction system's three-phase structure, may be limiting the reaction. Furthermore, these results have significant ramifications for the synthesis of biodiesel on an industrial and laboratory scale. Clear optimization criteria for both MeOH and catalyst have been demonstrated. Thus, offering useful recommendations for effective process design.

The intricate interactions between reactant ratios (oil:methanol:NaOH), reaction temperature (a), and time on biodiesel yield (b) are shown in Fig. 1 (a and b). Due to the transesterification reaction's kinetic restrictions, yields at low temperatures (30–50°C) are still somewhat low (35–70%) for all reactant ratios. This behaviour is explained by the Arrhenius equation [23], which states that molecule collisions and reaction rates are limited by a lack of heat energy. It's interesting to note that even at 30°C, the 1:3:0.05 ratio (B7) yields 49%, which is much greater than the 1:0.5:0.01 ratio's 35% yield (B1). This emphasizes how crucial extra methanol and a suitable catalyst are for breaking through low-temperature kinetic barriers. As the temperature increases to 60–70°C, yields improve dramatically, peaking at 97% for the 1:3:0.05 ratio (B7) at 70°C. This optimal performance aligns with methanol's boiling point (~ 65°C), where increased thermal energy enhances mass transfer and reaction kinetics without excessive methanol loss. The data also reveal that catalyst concentration plays a decisive role: while the 1:3:0.01 ratio (B6) achieves 90% yield at 70°C, increasing the catalyst to 0.05 w/w (B7) boosts the yield to 97%. Beyond this point, further catalyst

increases (B8-B15) do not significantly improve yields, suggesting a threshold where active site availability becomes non-limiting. Interestingly, at elevated temperatures (80–160°C), yields stabilize but show a slight decline in some cases. For example, the 1:3:1 ratio (B15) drops from 89% at 100°C to 85% at 160°C, likely due to thermal degradation of FAMEs or catalyst deactivation. However, the 1:3:0.05 ratio (B7) maintains a robust 94–95% yield even at 160°C, demonstrating superior thermal stability. This suggests that optimized reactant ratios can mitigate high-temperature inefficiencies, possibly by reducing side reactions like saponification [22].

At short reaction times (20–30 min) Fig. 1 (b), yields remain low (9–40%) across all conditions, reflecting incomplete conversion due to kinetic limitations. However, the 1:3:0.13 ratio (B9) shows relatively faster kinetics, reaching 40% yield at 30 min compared to just 25% for the 1:0.5:0.01 ratio (B1). This acceleration can be attributed to sufficient methanol availability and optimal NaOH concentration (0.13 w/w), which enhances the formation of methoxide ions while minimizing soap formation. The most dramatic improvements occur between 40–60 min, where yields increase exponentially. The 1:3:0.05 ratio (B7) achieves 97% yield at 60 min/70°C - the highest observed conversion. This combination represents the thermodynamic and kinetic optimum where [24]: (i) Methanol excess (3:1 ratio) drives equilibrium toward FAME production; (ii) Moderate NaOH (0.05 w/w) provides sufficient catalytic sites without excessive saponification; (iii) 60–70°C temperature enhances mass transfer while preventing methanol evaporation; (iv) 60 min duration allows complete conversion without product degradation. Notably, yields plateau or slightly decrease beyond 60 min, particularly for high NaOH loadings (> 0.15 w/w). The 1:3:1 ratio (B15) drops from 94% at 60 min to 85% at 90 min, likely due to reverse reactions from glycerol accumulatio or Soap formation consuming FAME products.

Temperature effects follow similar trends to previous findings, with 70°C remaining optimal. However, the time data reveal that lower temperatures (50–60°C) can achieve comparable yields if reaction times are extended sufficiently. For instance, the 1:3:0.05 system reaches: 82% at 60 min/60°C, 97% at 60 min/70°C, and 90% at 90 min/50°C. This presents an important trade-off between energy input (temperature) and processing time for industrial applications.

The analysis of trace metal concentrations in mechanically pressed *Jatropha curcas* oil from Sudan and its biodiesel and glycerol derivatives reveals important patterns in elemental partitioning during biofuel production (Table 2). Sodium emerges as the predominant contaminant, with concentrations of 10.2 ppm in crude oil and 10 ppm in biodiesel, suggesting significant carryover during processing. This sodium likely originates from equipment contact or water used in washing, as evidenced by its minimal transfer to glycerol (0.2 ppm), indicating poor solubility in the polar byproduct.

Table 2
Elements Composition in Jatropha curcas Oil, Biodiesel, and Glycerol Characterized by ICP

Element	Concentration in ppm		
	Oil	Biodiesel (B7)	Glycrol
Na	6	5.8	0.2
Mg	2.1	1.8	0.3
Al	3	2.4	0.6
Fe	5.5	4	1.5
Ni	2	0.7	1.3
Cu	1.8	0.3	1.5
V	1.3	0.2	1.1
As	1.2	0.3	0.9

Transition metals exhibit varied behavior across the production chain. Iron maintains relatively high levels in both oil (5.5 ppm) and biodiesel (4 ppm), while nickel shows moderate retention in biodiesel (0.7 ppm from 2 ppm in oil). These findings are particularly concerning as both metals are known to catalyze oxidative degradation in biodiesel [25]. Copper and vanadium demonstrate preferential partitioning into glycerol (1.5 ppm and 1.1 ppm respectively), likely forming complexes during transesterification. The presence of arsenic at 1.2 ppm in crude oil, with 0.3 ppm remaining in biodiesel, suggests potential soil contamination in the Sudanese cultivation regions and warrants further investigation into agricultural practices.

The data reveal that alkaline earth metals magnesium and aluminum show intermediate behavior, with significant portions transferring to glycerol (0.3 ppm and 0.6 ppm respectively), consistent with their known soap-forming tendencies during biodiesel production. This partitioning behavior has important implications for purification processes, as these metals can affect catalyst performance and final fuel quality. These findings highlight several quality control challenges specific to Jatropha biodiesel production. The elevated sodium and iron levels particularly emphasize the need for improved processing techniques or additional purification steps to meet international biodiesel standards. The presence of potentially toxic elements like arsenic and vanadium, though at relatively low concentrations, suggests the importance of monitoring soil conditions in cultivation areas and implementing metal-specific removal strategies during refining.

The highest-quality biodiesel sample (B7), produced under optimal reaction conditions, was further enhanced using gamma irradiation at varying doses (3, 6, 10, 15, 18 and 20 kGy) with dose rates of 2.27, 4.5, 7.4, 11.15, 14.1 and 16.8 kGy/h, respectively. This post-treatment aimed to modify the fuel's physicochemical properties and fatty acid methyl ester (FAME) profile, which directly influence biodiesel performance, stability, and compliance with international standards (ASTM).

To evaluate the irradiation effects, comprehensive gas chromatography (GC/MS) analysis was conducted to quantify FAME composition before and after exposure. Additionally, key fuel properties—including density (D4052), rinematic viscosity (D7042), flash point (D93), cloud point (D5773), color (D1500), ash content (D482), water content (D95), carbon residue (D4530), sulfur content (D5453), copper strip corrosion (D130), and cetane number (D6131)—were systematically assessed at each radiation dose. Gamma irradiation is known to induce radiolytic cleavage of peroxides and double bonds in unsaturated FAMEs, potentially improving oxidative stability and cold-flow properties [26]. However, excessive doses may promote degradation, necessitating careful optimization of irradiation parameters for maximal benefit [26].

Table 3
Effect of Gamma Irradiation Dose on Biodiesel Yield and Fatty Acid Methyl Ester (FAME) Composition

Dose (kGy)	yield % of FAMEs						
	Total biodiesel yield	Methyl palmitoleate (C16:1)	Methyl palmitate (C16:0)	Methyl heptadecanoate (C17:0)	Methyl elaidate C18:1 trans	Methyl dihydrosterculate (C19:0 cyclo)	Methyl cerotate (C26:0)
0	97	15	20	12	35	10	5
6	97	13	22	10	38	8	6
10	99	15	25	10	40	4	5
15	90	13	21	9	33	6	8
18	89	14	20	10	31	6	8
20	87	16	22	11	30	4	4

This investigation In Table 3 reveals significant effects of gamma irradiation (0–20 kGy/h) on biodiesel production efficiency and fatty acid methyl ester (FAME) stability. The study demonstrates an optimal irradiation range that enhances production while identifying critical degradation thresholds that impact fuel quality. At moderate doses (6–10 kGy), irradiation improves transesterification efficiency, evidenced by peak biodiesel yields of 97–98%. This enhancement correlates with increased methyl elaidate (C18:1 trans) content from 35% to 40%, suggesting radiation-induced cis-trans isomerization of unsaturated bonds. The process appears mediated by free radical mechanisms that temporarily improve reaction kinetics without immediate structural damage. However, irradiation beyond 15 kGy initiates progressive degradation, with yields declining to 87% at maximum dose. Three primary degradation pathways emerge: (i) Oxidative cleavage preferentially targets unsaturated FAMEs, particularly evident in methyl elaidate reduction from 40% to 30% at higher doses. Comparative stability tests show irradiated samples experience 15–20% greater unsaturated FAME loss than non-irradiated controls during accelerated aging. (ii) Cyclopropane ring opening occurs in methyl dihydrosterculate (C19:0 cyclo), with content halving from 10% to 4–6% under irradiation. This suggests gamma exposure induces homolytic cleavage of strained cyclic structures. (iii) Polymerization and ester scission become dominant at doses exceeding 15 kGy, confirmed by increasing high-molecular weight byproducts and reduced biodiesel yield.

The data in Fig. 2 reveal significant dose-dependent changes in fatty acid methyl ester (FAME) selectivity during gamma irradiation-assisted biodiesel production. At 0 kGy, the FAME profile shows expected natural distribution, with methyl elaidate (C18:1 trans, 36.1%) and methyl palmitate (C16:0, 20.6%) as dominant components. As irradiation increases to 10 kGy, several notable trends emerge: (i) Unsaturated FAME Isomerization: Methyl elaidate content peaks at 40.8% (10 kGy), suggesting gamma radiation promotes cis-to-trans isomerization of monounsaturated bonds [26–28]. This is accompanied by a concurrent decrease in methyl palmitoleate (C16:1) from 15.5% to 14.3%,

indicating preferential modification of olefinic bonds under irradiation. (ii) Saturated FAME Enhancement: Methyl palmitate (C16:0) increases from 20.6% to 25.5% at 10 kGy, likely through hydrogenation of radical intermediates or stabilization of saturated chains against radiolytic cleavage. (iii) Cyclopropane Ring Degradation: Methyl dihydrosterculate (C19:0 cyclo) shows progressive decline from 10.3% to 4.1% at 10 kGy, demonstrating radiation sensitivity of cyclopropane structures through potential ring-opening mechanisms [26, 28].

The system displays radiation saturation effects beyond 10 kGy/h: (a) methyl elaidate drops to 34.5% (20 kGy/h), indicating that at higher doses, oxidative degradation takes precedence over isomerization; (b) methyl cerotate (C26:0) behaves non-linearly, potentially as a result of competing long-chain radical fragmentation and recombination; and (c) the apparent recovery of methyl palmitoleate at 20 kGy/h (18.4%) might be a sign of secondary radical recombination products. These results, however, indicate that gamma irradiation at dosages below 10 kGy/h causes gradual deterioration, but gamma irradiation at higher levels selectively alters FAME profiles through radical-mediated pathways [26, 29]. By balancing advantageous isomerization effects against harmful oxidative pathways, the ideal 6–10 kGy/h range offers a viable tool for controlling irradiation and customizing the characteristics of biodiesel. Figure 3 reports the effects of gamma irradiation on the physicochemical characteristics of biodiesel (B7).

While following to ASTM standards, the effects of gamma irradiation dosages (0–20 kGy) on important biodiesel quality metrics show notable changes in physicochemical attributes. Radiation-induced molecular fragmentation, especially in heavier hydrocarbon chains, is suggested by the steady reduction in density (Fig. 3a) from 0.89 g/mL (0 kGy) to 0.86 g/mL (10 kGy), which stabilizes at higher doses. As seen by the parallel viscosity trend where kinematic viscosity hits its minimum (4.3 mm^2/s at 10 kGy), this 3.4% reduction is consistent with the radiolytic cleavage of unsaturated FAMEs and represents a 28% improvement over the control sample (Fig. 3b). Furthermore, despite irradiation, the flash point constantly stays above 152°C for all doses (Fig. 3c), above the ASTM minimum of 93°C by 64%, indicating maintained safety [27]. Furthermore, cloud point fluctuates very little (0.70–0.90°C) and does not exhibit a distinct dose-dependent pattern, indicating that molecular weight distribution, not FAME saturation, is the primary effect of gamma irradiation (Fig. 3d). Supported by steady corrosion characteristics, the persistent light colour (1.5 on the ASTM scale) verifies the lack of significant oxidative deterioration (Fig. 3e). Although it marginally increases at higher doses as secondary radiolytic products occur, the ash content shows an ideal reduction at 10 kGy (0.015%, 50% lower than control) (Fig. 3f), most likely due to radiation-assisted destruction of metallic impurities. Also, changes in water content (0.030–0.052%) stay within ASTM limits (≤ 0.05%) (Fig. 3g), suggesting that radiation has no discernible effect on hygroscopicity [30]. Additionally, we observed that the sulphur content (4.6–5 ppm, much below the 15 ppm limit) and copper strip corrosion rating (1a) were steady, indicating that gamma treatment did not introduce corrosive elements or sulfur-based oxidation products [31].

However, the 10 kGy dose, shows the best combination of properties. Comparative study with ASTM criteria, demonstrates that all irradiated samples meet key specifications. These results indicate that regulated gamma irradiation (≤ 15 kGy) can improve the fluidity of biodiesel without affecting other quality indicators; nevertheless, dosage optimization is necessary to balance the effects of fragmentation and repolymerization. In particular, the data suggest the use of irradiation as a post-treatment for high-viscosity feedstocks, where a dose of 10 kGy may enhance flow characteristics while maintaining standards for fuel safety and purity. Figure 4 shows the effect of the dose of Gamma Irradiation on the Cetane Number of Biodiesel.

The cetane number (CN), a critical parameter reflecting biodiesel's ignition quality [28], demonstrates a clear dependence on gamma irradiation dose, as evidenced by the non-linear trend observed in the experimental data (Fig. 4). The initial increase in CN from 50 (0 kGy) to 57 (10 kGy) suggests that moderate gamma irradiation (6–10 kGy) induces favorable molecular modifications in the biodiesel's fatty acid methyl ester (FAME) profile. This improvement likely stems from radiolytic fragmentation of long-chain unsaturated FAMEs, which generates shorter, more saturated hydrocarbon fragments known to enhance ignition characteristics. The peak CN at 10 kGy coincides with the previously reported minimum viscosity (4.3 mm^2/s) from parallel studies, reinforcing that radiation-induced breakdown of bulky triglyceride derivatives improves both fuel atomization and combustion efficiency.

Moreover, at higher doses (15–20 kGy), the subsequent decline in CN (51–49) implies competing molecular recombination effects, where radiation-generated free radicals form branched or cyclic compounds that hinder optimal combustion. This trend aligns with the observed rebound in viscosity at these doses, as repolymerization creates molecular structures with slower oxidation kinetics. Notably, even at the highest dose (20 kGy), the CN (49) remains above the ASTM D6751 minimum (≥ 47), confirming that gamma irradiation does not compromise compliance with industrial standards. The temporary CN enhancement at 10 kGy offers dual environmental advantages: (1) Reduced greenhouse gas emissions due to more complete combustion (lower CO and unburned hydrocarbon output), and (2) Better cold-start performance, which minimizes the energy-intensive preheating required for high-viscosity biodiesel in cold climates. The absence of chemical additives in this process—unlike conventional CN boosters (e.g., 2-ethylhexyl nitrate)—makes gamma irradiation a cleaner modification technique. However, the dose-dependent effects underscore the need for precise optimization, as excessive radiation (≥ 15 kGy) diminishes these benefits while unnecessarily increasing energy input.

Future studies should couple CN measurements with detailed FAME profiling (e.g., GC-MS) to quantify radiation-induced saturation of oleic (C18:1) and linoleic (C18:2) acids, which are primary contributors to CN variation. Additionally, life-cycle assessment (LCA) of the irradiation process would clarify its net environmental footprint compared to alternative CN improvement methods. This dataset provides foundational evidence that controlled gamma irradiation (≤ 10 kGy) could serve as a scalable post-production treatment to upgrade biodiesel ignition quality without synthetic additives, aligning with global mandates for cleaner, high-performance renewable fuels.

Conclusion

This study successfully optimized biodiesel production from *Jatropha curcas* oil, achieving a 97% yield under ideal transesterification conditions (30g methanol, 0.5g NaOH, 70°C, 60 min). Post-production gamma irradiation (6–10 kGy) further enhanced fuel properties, improving viscosity, cetane number, and oxidative stability without compromising ASTM compliance. However, excessive irradiation (> 15 kGy) induced degradation, reducing yield and altering fatty acid profiles. The findings highlight the potential of *Jatropha curcas* as a sustainable biodiesel feedstock, with gamma irradiation serving as a viable post-treatment to refine fuel quality. Future research should explore large-scale applications and environmental impacts of irradiation to optimize industrial adoption. This work contributes to advancing renewable energy solutions by integrating process optimization and innovative modification techniques for improved biodiesel performance.

Declarations

Disclosure Statement

No potential conflict of interest was reported by the author(s).

Data Availability Statement

The original contributions presented in the study are included in the article material, further inquiries can be directed to the corresponding author.

References

1. Nayab, R., Imran, M., Ramzan, M., et al.: Sustainable biodiesel production via catalytic and non-catalytic transesterification of feedstock materials: a review. Fuel. **328**, 125254 (2022). 10.1016/j.fuel.2022.125254
2. Ahmad, A., Yasin, N.M., Derek, C., et al.: Microalgae as a sustainable energy source for biodiesel production: a review. Renew. Sust Energ. Rev. **15**, 584–593 (2011). 10.1016/j.rser.2010.09.018
3. Kafuku, G., Mbarawa, M.: Biodiesel production from Croton megalocarpus oil and its process optimization. Fuel. **89**, 2556–2560 (2010). 10.1016/j.fuel.2010.03.039
4. Glisic, S.B., Pajnik, J.M., Orlović, A.M.: Process and techno-economic analysis of green diesel production from waste vegetable oil and the comparison with ester type biodiesel production. Appl. Energ. **170**, 176–185 (2016). 10.1016/j.apenergy.2016.02.102
5. Demir, V., Akgün, M.: New catalysts for biodiesel production under supercritical conditions of alcohols: a comprehensive review. ChemistrySelect. **7**, e202104459 (2022). 10.1002/slct.202104459
6. Yan, S., Salley, S.O., Simon Ng, K.Y.: Simultaneous transesterification and esterification of unrefined or waste oils over ZnO-La_2O_3 catalysts. Appl. Catal. Gen. **353**, 203–212 (2009). 10.1016/j.apcata.2008.10.053
7. Deshpande, S.R., Sunol, A.K., Philippidis, G.: Status and prospects of supercritical alcohol transesterification for biodiesel production. Wiley Interdiscip Rev. Energy Environ. **6**, e252 (2017). 10.1002/wene.252
8. Bernal, J.M., Lozano, P., García-Verdugo, E., et al.: Supercritical synthesis of biodiesel. Molecules. **17**, 8696–8719 (2012). 10.3390/molecules17078696
9. Tan, K.T., Gui, M.M., Lee, K.T., Mohamed, A.R.: Supercritical alcohol technology in biodiesel production: a comparative study between methanol and ethanol. Energy Sources Part. A. **33**, 156–163 (2011). 10.1080/15567030902937226
10. Fazal, M., Haseeb, A., Masjuki, H.: Biodiesel feasibility study: an evaluation of material compatibility, performance, emission and engine durability. Renew. Sust Energ. Rev. **15**, 1314–1324 (2011). 10.1016/j.rser.2010.10.004
11. Silitonga, A., Atabani, A., Mahlia, T., et al.: A review on *prospect of Jatropha curcas for biodiesel in Indonesia*. Renew Sust Energ. Rev. **15**, 3733–3756 (2011). 10.1016/j.rser.2011.07.011
12. Marulanda, V.F.: Biodiesel production by supercritical methanol transesterification: process simulation and potential environmental impact assessment. J. Clean. Prod. **33**, 109–116 (2012). 10.1016/j.jclepro.2012.04.022

13. Shin, H.Y., Lee, S.H., Ryu, J.H., et al.: Biodiesel production from waste lard using supercritical methanol. J. Supercrit Fluids. **61**, 134–138 (2012). 10.1016/j.supflu.2011.09.009
14. Naik, M., Meher, L.C., Naik, S.N., Das, L.M.: Production of biodiesel from high free fatty acid Karanja (Pongamia pinnata) oil. Biomass Bioenergy. (2007). 10.1016/j.biombioe.2007.10.006
15. Kusdiana, D., Saka, S.: Effects of water on biodiesel fuel production by supercritical methanol treatment. Bioresource Technol. **91**, 289–295 (2004). 10.1016/S0960-8524(03)00201-3
16. Bhansali, K.J., Bhagat, P.R.: Production of Furfural-Diethyl-Acetal as Biofuel Additives for Gasoline by Metal Free Porphyrin Photocatalyst Under Visible Light. Catal. Lett. **152**, 2386–2400 (2022). 10.1007/s10562-021-03809-z
17. Ezeldin Osman, M.E., Sheshko, T.F., Dipheko, T.D., et al.: Synthesis and improvement of Jatropha curcas L. biodiesel based on eco-friendly materials. Int. J. Green. Energy. **18**(13), 1396–1404 (2021). 10.1080/15435075.2021.1904943
18. Sander, K., Murthy, G.S.: Life cycle analysis of algae biodiesel. Int. J. Life Cycle Assess. **15**, 704–714 (2010). 10.1007/s11367-010-0194-1
19. Osman, M.E., Younis, F., Elamin, A.A., et al.: Improvement the Physico-chemical Characteristics of Diesel Fuel using Gamma Irradiation. J. Mex Chem. Soc. **65**(4), 2594–0317 (2021). 10.29356/jmcs.v65i4.1552
20. Hillert, M.: Le Chatelier's principle—restated and illustrated with phase diagrams. JPE. **16**, 403–410 (1995). 10.1007/BF02645347
21. Pasha, M.K., Dai, L., Liu, D., et al.: An overview to process design, simulation and sustainability evaluation of biodiesel production. Biotechnol. Biofuels. **14**, 129 (2021). 10.1186/s13068-021-01977-z
22. Singh, D., Sharma, D., Sharma, P.K., et al.: Characterization of homogenous acid catalyzed biodiesel production from palm oil: experimental investigation and numerical simulation. Environ. Sci. Pollut Res. **30**, 34481–34502 (2023). 10.1007/s11356-022-24515-2
23. Martín-Martín, R., Dorta-Guerra, R., Torsney, B.: Multiplicative algorithm for discriminating between Arrhenius and non-Arrhenius behaviour. Chemometr Intell. Lab. Syst. **139**, 146–155 (2014). 10.1016/j.chemolab.2014.10.001
24. Kaisan, M.U., Abubakar, S., Ashok, B., et al.: Comparative analyses of biodiesel produced from jatropha and neem seed oil using a gas chromatography–mass spectroscopy technique. Biofuels. (2018). 10.1080/17597269.2018.1537206
25. Sharma, Y.C., Singh, B., Upadhyay, S.N.: Advancements in development and characterization of biodiesel: a review. Fuel. **87**, 2355–2373 (2008). 10.1016/j.fuel.2008.01.014
26. Jongput, B., Chiwpreecha, P., Ruangsomboon, S., et al.: Enhancing biomass, hydrocarbon and biodiesel properties of green microalga Botryococcus braunii KMITL through gamma and UV radiation exposure. Sci. Rep. **14**, 24684 (2024). 10.1038/s41598-024-76576-7
27. Yoon, M., Jong-il, C., Gwang, H.K., et al.: Proteomic analysis of Spirogyra varians mutant with high starch content and growth rate induced by gamma irradiation. Bioproc Biosys Eng. **36**, 765–774 (2013). 10.1007/s00449-013-0902-x
28. Knothe, G.: Improving biodiesel fuel properties by modifying fatty ester composition. Energy Environ. Sci. **2**, 759–766 (2009). 10.1039/B903941D
29. Chakravarty, B., Sen, S.: Enhancement of regeneration potential and variability by gamma irradiation in cultured cell of Scilla Indica. Biol. Plant. **44**, 193–199 (2001). 10.1023/A:1010282805522
30. Maroa, S., Inambao, F.: Physicochemical Properties of Biodiesel. In: Biodiesel, Combustion, Performance and Emissions Characteristics. Green Energy and Technology. *Springer, Cham*; (2020). 10.1007/978-3-030-51166-1_5
31. Ezeldin, M., Masaad, A.M., Abualreish, M.J.A., Ishak, C.Y.: The Role of Isopropyl Alcohol in the Properties of Sudanese Reformat Gasoline. Orient. J. Chem. **33**(4), 2085–2089 (2017). 10.13005/ojc/330458

Figures

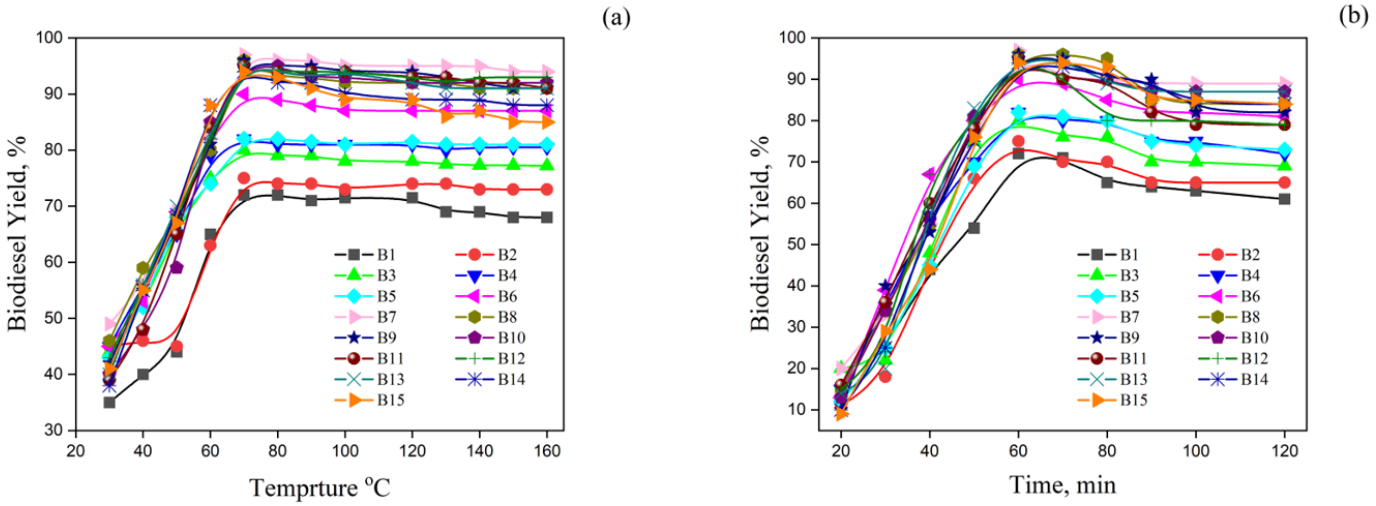

Figure 1

Dependence of Biodiesel Yield at different [Oil: Methanol: Catalyst] ratios (B1-15) on: ***(a)*** Reaction Temperature (°C) for 60; ***(b)*** Reaction Time (Minutes).

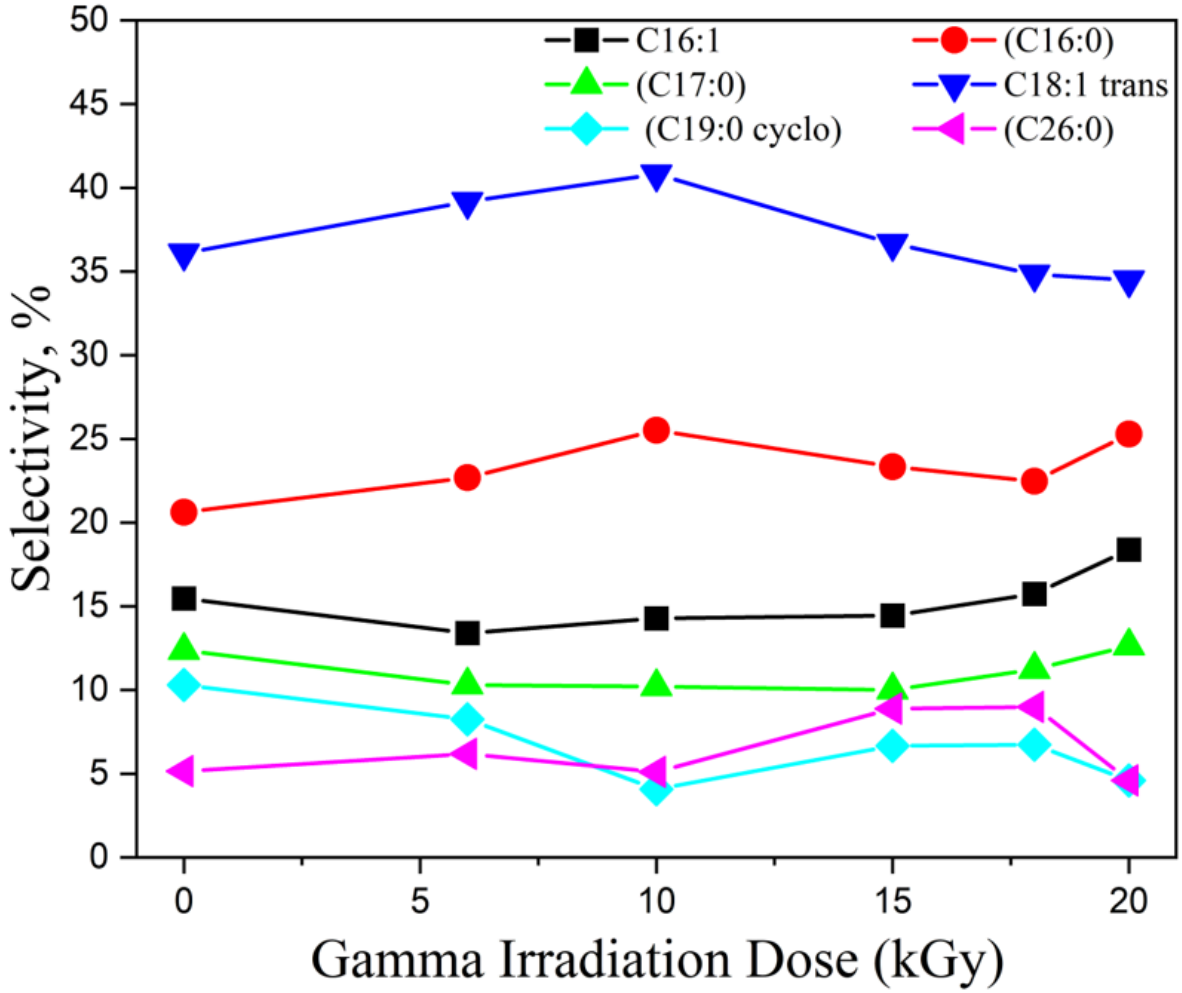

Figure 2

Gamma Irradiation Effects on Fatty Acid Methyl Ester Selectivity in Biodiesel Production. (C16:1) — Methyl palmitoleate; (C16:0) —Methyl palmitate; (C17:0) —Methyl heptadecanoate; (C18:1 trans) —Methyl elaidate; (C19:0 cyclo) —Methyl dihydrosterculate; (C26:0) —Methyl cerotate.

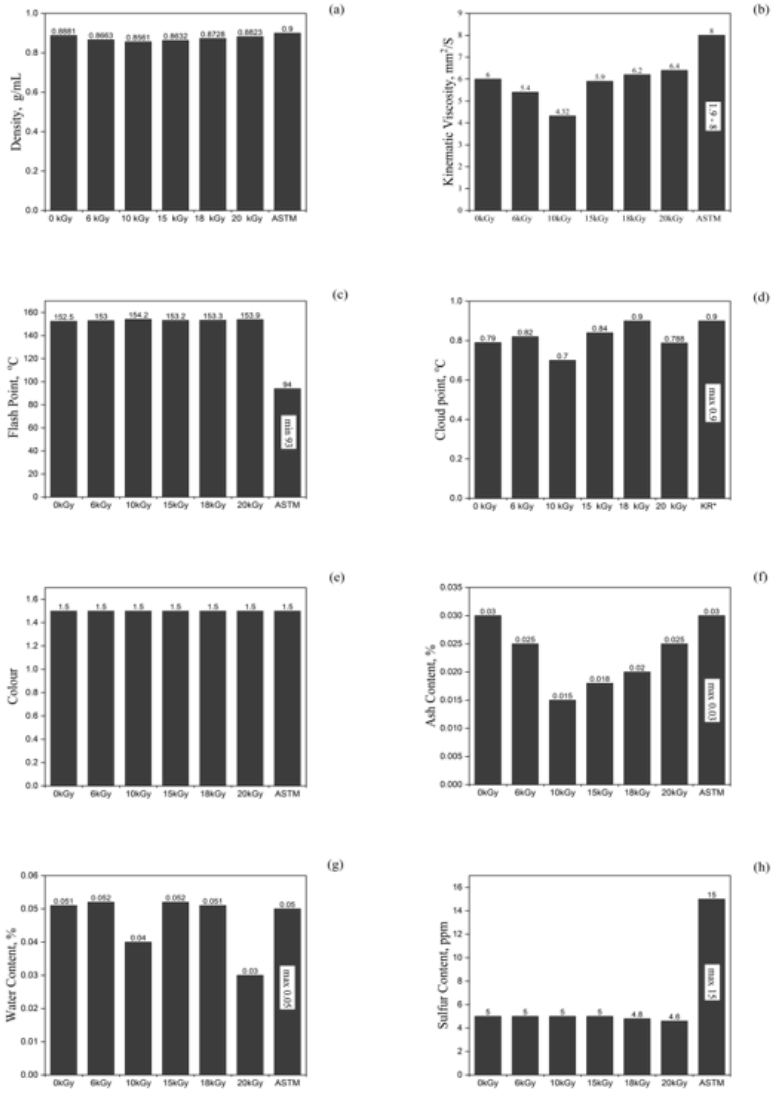

Figure 3

Gamma Irradiation Dose's Impact on Important Biodiesel Physicochemical Properties in Contrary to ASTM Standards: ***(a)***Density (g/mL), ***(b)*** Kinematic Viscosity (mm²/s); ***(c)*** Flash Point (°C); ***(d)***Cloud Point (°C), ***(e)*** Colour (ASTM Scale); ***(f)*** Ash Content (%), ***(g)***Water Content (%); ***(h)*** Sulfur Content (ppm)

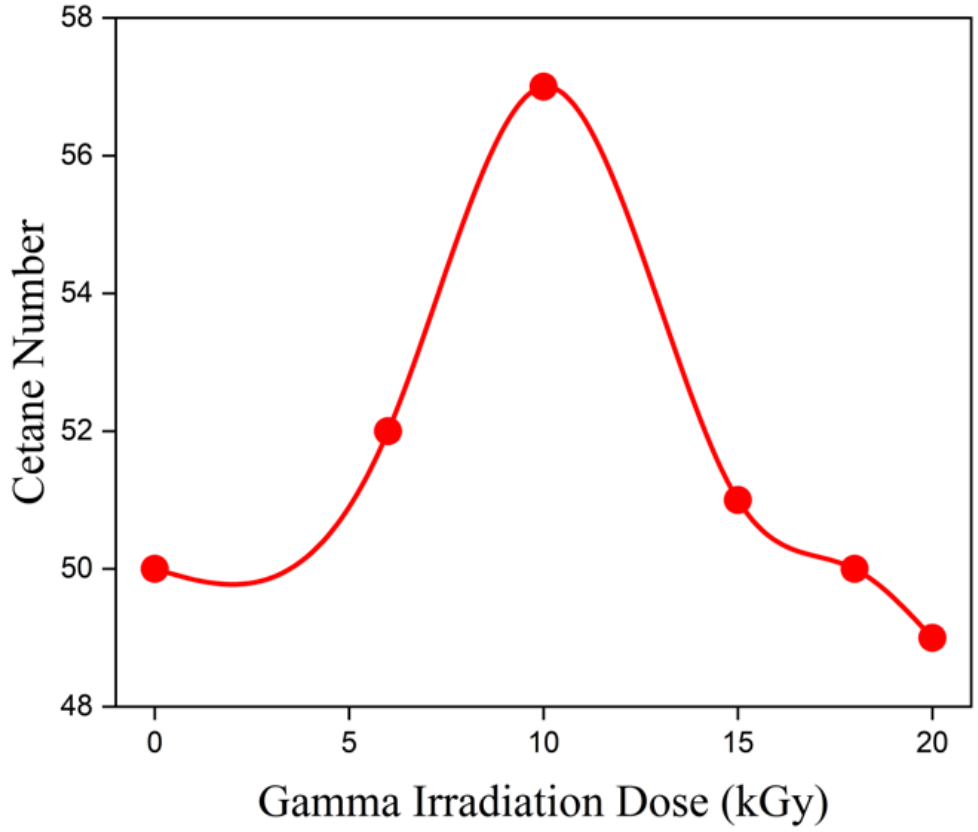

Figure 4

Impact of Gamma Irradiation Dose on the Cetane Number of Biodiesel: Correlations Between Radiation-Induced Molecular Modifications and Combustion Performance